

The energy distribution of the initial photons given by the integrand of Eq. (1) is strongly peaked at low photon energies. Thus, at the end of several steps of a typical photon cascade, neutron emission will be possible, removing such nuclei from detectability in this experiment. We estimate that the decay of the gold nucleus can proceed by initial photon emission in as many as one-third of the photonuclear excitations.

- ¹ Keck, Stearns, and Wilson, *Phys. Rev.* **79**, 199 (1950).
- ² E. R. Gaertner and M. L. Yeater, *Phys. Rev.* **76**, 363 (1949).
- ³ Dressel, Goldhaber, and Hanson, *Phys. Rev.* **77**, 754 (1950).
- ⁴ M. Goldhaber and E. Teller, *Phys. Rev.* **74**, 1046 (1948).
- ⁵ G. C. Baldwin and G. S. Klaiber, *Phys. Rev.* **70**, 259 (1946).
- ⁶ R. Sagane, *Phys. Rev.* **83**, 174 (1951).
- ⁷ L. Katz and A. G. W. Cameron, *Phys. Rev.* **83**, 892 (1951), and to be published.
- ⁸ Johns, Katz, Douglas, and Haslam, *Phys. Rev.* **80**, 1062 (1950).
- ⁹ Hüber, Humbel, Schneider, de Shalit, and Zunti, *Helv. Phys. Acta* **24**, 127 (1951).
- ¹⁰ L. Katz and A. G. W. Cameron, *Can. J. Phys.*, to be published.
- ¹¹ A. G. W. Cameron, *Phys. Rev.* **82**, 272 (1951).
- ¹² J. S. Levinger and H. A. Bethe, *Phys. Rev.* **78**, 115 (1950).
- ¹³ J. M. Blatt and V. F. Weisskopf, privately circulated notes to appear as Chapter XII in their book, *Theoretical Nuclear Physics*.
- ¹⁴ V. F. Weisskopf, in *Lecture Series in Nuclear Physics*, (U. S. Government Printing Office, Washington, D. C., 1947), MDDC 1175, p. 104.

Conductivity of the Sodium Tungsten Bronzes*

B. W. BROWN AND E. BANKS
Polytechnic Institute of Brooklyn, Brooklyn, New York
(Received September 12, 1951)

RECENT work by Straumanis and Dravnieks¹ and Huibregtse, Barker, and Danielson² has shown that the cubic sodium tungsten bronzes (Na_xWO_3 , where x varies between 0.95 and 0.3) have high electrical conductivity. These workers found a positive temperature coefficient of resistivity, but the conclusion that the conductivity was metallic in nature was not justified by their data, which did not show a linear dependence of resistivity upon temperature. This linear temperature dependence would be expected from the free electron model proposed by Stubbin and Mellor³ and Kupka and Sienko⁴ on the basis of magnetic susceptibility measurements. The magnitude of the conductivity reported previously appeared too low to fit in with a free electron picture, and gave a value for the mobility of electrons, as calculated by Huibregtse, *et al.*, which was smaller than that of metallic sodium by a factor of twenty-four.

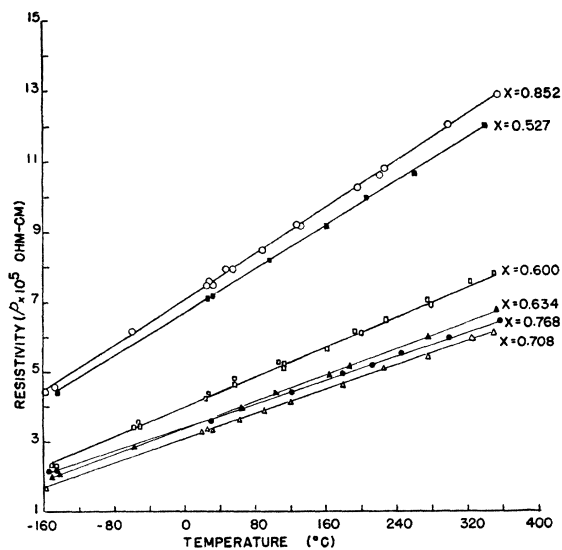


FIG. 1. Plot of resistivity vs temperature for six compositions of sodium tungsten bronze, Na_xWO_3 .

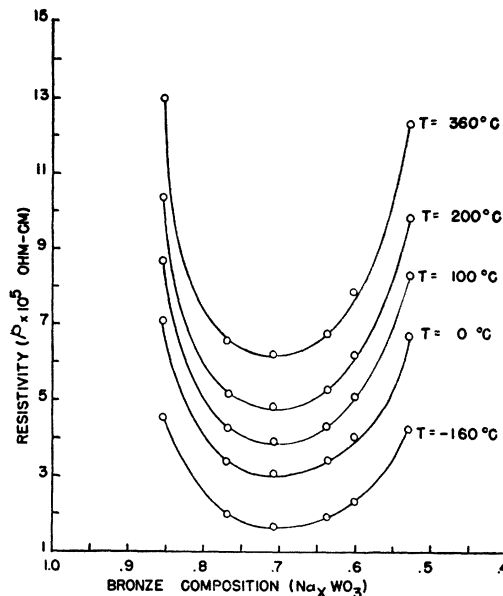


FIG. 2. Resistivity isotherms for various sodium tungsten bronzes.

The measurements reported here were made by a potential probe method (to eliminate contact effects) over a temperature range of -160° to $+360^\circ\text{C}$, for single crystals of six different compositions. The results, shown in Fig. 1, indicate a linear temperature dependence of resistivity over the entire temperature range studied. This is quantitative confirmation of the metallic nature of conduction in these materials. Using our value for the conductivity of $\text{Na}_{0.708}\text{WO}_3$ ($3.0 \times 10^4 \text{ ohm}^{-1}\text{cm}^{-1}$ at 25°C) and the value obtained by Huibregtse, *et al.* for the Hall coefficient of $\text{Na}_{0.685}\text{WO}_3$ ($-5.3 \times 10^{-4} \text{ cm}^3/\text{coulomb}$ at 25°C), we obtain an electron mobility of $16 \text{ cm}^2/\text{volt-sec}$ as compared with $2 \text{ cm}^2/\text{volt-sec}$ calculated by Huibregtse, *et al.* and $48 \text{ cm}^2/\text{volt-sec}$ reported for metallic sodium. It appears that the mobility of electrons in these bronzes is approximately 35 percent of their mobility in metallic sodium.

In Fig. 2 a series of resistivity isotherms is shown as a function of bronze composition. The compositions were determined by x-ray analysis of powdered bronzes heated in contact with a single crystal until composition equilibrium was obtained. These compositions have lattice constants that fall on the linear portion of a lattice constant—composition curve of a previously prepared series of powdered bronzes.⁵ These isotherm curves show a minimum in resistivity at approximately $x=0.70$. The temperature coefficients of resistivity behave in a similar manner (Table I).

We propose a tentative interpretation of this resistivity minimum in terms of equilibrium between undissociated sodium atoms and sodium ions plus free electrons. In the region below $x=0.70$ each sodium atom introduced contributes one free electron and one random scattering center (Na^+); while above $x=0.70$ the addition of undissociated sodium atoms contributes only additional scattering centers. These additional scattering centers are

TABLE I. Resistivity of sodium tungsten bronzes— Na_xWO_3 .

Composition	Resistivity		Temp. coef. of resist. ohm-cm per $^\circ\text{C}$
	Temp. ($^\circ\text{C}$)	$\rho \times 10^5$	
$x=0.852$	26.5	7.50 ± 0.04	16.33×10^{-8}
$x=0.768$	27.5	3.65 ± 0.03	8.75×10^{-8}
$x=0.708$	29.0	3.34 ± 0.02	8.40×10^{-8}
$x=0.634$	27.0	3.67 ± 0.03	9.38×10^{-8}
$x=0.600$	26.0	4.50 ± 0.04	10.62×10^{-8}
$x=0.527$	31.0	7.18 ± 0.02	15.66×10^{-8}

presumed to be the cause of the increase of the resistivity as the sodium content is increased above $x=0.70$.

We wish to express our thanks to Professor J. J. Dropkin for numerous stimulating discussions.

* Supported by the Signal Corps.

¹ Straumanis and Dravnieks, J. Am. Chem. Soc. **71**, 683 (1949).

² Huibregtse, Barker, and Danielson, Phys. Rev. **82**, 770 (1951).

³ Stubbin and Mellor, Proc. Roy. Soc. N. S. Wales, **82**, 225 (1948).

⁴ F. Kupka and M. J. Sienko, J. Chem. Phys. **18**, 1296 (1950).

⁵ Th'rd Progress Report, Signal Corps contract (July 6, 1951), p. 5 (unpublished).

Capture and Scattering of π^+ Mesons*

G. BERNARDINI

Columbia University, New York, New York

AND

F. LEVY†

Palmer Physical Laboratory, Princeton University, Princeton, New Jersey

(Received September 17, 1951)

TO obtain a more complete survey on the nuclear interactions induced by pions in complex nuclei, plates (Ilford G5) were exposed to the π^+ beams of the Nevis Cyclotron as was previously done in the symmetric π^- beams.¹

The spreads in energy values of the π^+ beams are, respectively, 35–50 and 70–80 Mev. The relative occurrences of the two competing processes (stars and scatterings) in a total of 150 interactions found scanning “along the track” are indicated in Table I. We did not find any “stops in flight.”² In Table I, $\Sigma I'$ are total

TABLE I. Relative occurrence of stars and scattering.

Energy (in Mev)	$\Sigma I'$ (in cm)	Stars	Elastic scattering $>40^\circ$	Inelastic scattering	λ (in cm)
35–50	3120 ± 180	55	25	2	38 ± 4.5
70–80	2250 ± 100	63	16	9	25.5 ± 3

lengths of tracks and λ the evaluated mean free paths.¹ The first are corrected for the estimated electron and μ meson impurities.¹ The scatterings include some probable, but doubtful cases due to very steep tracks.

As in the π^- case the capture process predominates over the scatterings at both energies, but now the energy dependence of catastrophic processes (stars and inelastic scatterings) is more evident since the cross sections for star production by π^+ are respectively 0.38 and 0.67 barn, and the corresponding figures for π^- are 0.62 and 0.76. The origin of this difference between π^+ and π^- is not clear, but taking into account the energy dependence of the capture cross section a difference between $\lambda\pi^+$ and $\lambda\pi^-$ is expected as a result of the coulomb barrier. Some evaluations are in progress to estimate this effect.

The coulomb field could also explain the lack of strongly inelastic scatterings (frequently found with π^- of 70–100 Mev¹) in which the scattered π^+ meson has a very low energy ($E \lesssim 10$ Mev).

In Table II the frequencies of stars *versus* number of prongs are indicated. Because the features of these stars do not change ap-

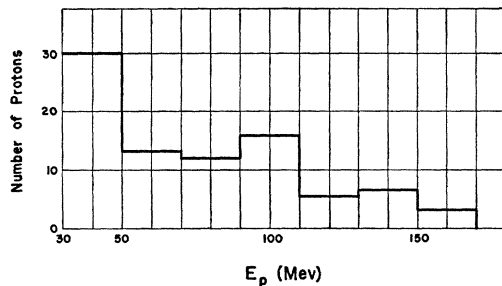


FIG. 1.

TABLE II. Frequencies of stars *vs* prongs.

No. prongs	0	1	2	3	4	5	6	7	Total
π^+	0	11(6)	32(20;6)	31(19;5)	18(11;2)	15(8;2)	6(3;2)	2(1;0)	115(68;17)
π^-	12	38(8)	27(8;0)	21(8;0)	4(0;0)	2(0;0)	0	0	104(24;0)

preciably between 50 and 100 Mev both energy ranges have been included in the table. The first figure enclosed by the parentheses are of those stars having one fast proton ($E \gtrsim 30$ Mev), the second figure, those having two fast protons. In a total of ~ 350 stars (including 150 stars found in “scanning per area”) all induced by π^- mesons, only one star with 2 fast proton prongs was observed. On the contrary, stars with 2 fast proton prongs represent more than 10 percent of ~ 250 (155 found “scanning per area”) π^+ captures. Table II also gives a simple explanation of the “stops in flight.” They are captures associated with the emission of neutrons only. Therefore, as was pointed out,³ they do not require the existence of a $\pi \rightarrow \pi^0$ scattering.

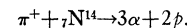
Considering the π^- capture as the mirror-image of the π^+ capture it is also possible to conclude that the charge-exchange scattering competes, if at all, only in a few percent in all π interactions. An energy-momentum balance of the π^+ stars allows as an upper limit for the $\pi \rightarrow \pi^0$ scattering a cross section not larger than $\frac{1}{10}$ of the total scattering cross section and $\approx 0.02\sigma$ geom. Wilson and Perry⁴ in a direct search for the scattered π^0 reach a similar conclusion in the light nuclei.

The frequencies of one and two fast proton stars give some support to the two-nucleon model recently discussed.⁵ With this model the probability of a π capture in nuclear matter can be written

$$W_c(\pi) = \Gamma \sigma(\pi^+ + d \rightarrow 2p).$$

Using the known value of σ ,⁶ Γ turns out to be of the order of 10. A more definite estimate of Γ would involve a quite questionable definition of the mean free path of pions in nuclear matter (we find, for π^+ of ~ 50 Mev, $\lambda \approx 3r_0$).

In some cases the two-nucleon absorption was evident because the two fast proton prongs show almost all the energy and momentum of the incoming π^+ . Two of these cases could be easily interpreted with the reaction scheme



The energy and angular distribution of fast protons emitted in π captures are given in Fig. 1 and Table III. They are preliminary results but they could possibly be of some use in the discussion of further meson experiments.

TABLE III. Angular distribution of fast protons in π -captures.

$(\theta, \pi p)$ in degrees	0–30	30–60	60–90	90–120	120–150	150–180
No. of fast protons	7	23	23	15	11	3

We are indebted to Messrs. J. Spiro, H. Edwards, and G. Rosenbaum for their assistance in the cyclotron operation and to Mesdames N. Bernardini and D. Lee for their invaluable help in scanning and measuring the nuclear events.

We owe very much to Dr. L. Lederman for his important contributions to this work, and Professor J. Steinberger for many interesting discussions.

* This work jointly sponsored by the ONR and AEC.

† On leave of absence from CNRS, Paris, France.

¹ Bernardini, Booth, Lederman, and Tinlot, Phys. Rev. **82**, 105 (1951); Bernardini, Booth, and Lederman, Phys. Rev. **83**, 1075 (1951).

² H. Bradner and B. Rankin, Phys. Rev. **80**, 916 (1950).

³ E. T. Booth, Meeting of the National Academy of Science, Washington, April, 1951; Bernardini, Booth, and Lederman, Phys. Rev. **83**, 1975 (1951).

⁴ Kindly communicated by R. Wilson and J. P. Perry.

⁵ Brueckner, Serber, and Watson, University of California Radiation Laboratory, 1358 (1951).

⁶ Durbin, Loar, and Steinberger, Phys. Rev. **83**, 646 (1951); Clark, Roberts, and Wilson, Phys. Rev. **83**, 649 (1951); Phys. Rev. (to be published); (kindly sent by the above authors).